Research Article

Yun-Fei Zhang, Fei-Peng Du*, Ling Chen, Ka-Wai Yeung, Yuqing Dong, Wing-Cheung Law, Gary Chi-Pong Tsui, and Chak-Yin Tang*

Supramolecular ionic polymer/carbon nanotube composite hydrogels with enhanced electromechanical performance

https://doi.org/10.1515/ntrev-2020-0039
received April 02, 2020; accepted April 07, 2020

Abstract: Electroactive hydrogels have received increasing attention due to the possibility of being used in biomimetics, such as for soft robotics and artificial muscles. However, the applications are hindered by the poor mechanical properties and slow response time. To address these issues, in this study, supramolecular ionic polymer–carbon nanotube (SIPC) composite hydrogels were fabricated via *in situ* free radical polymerization. The polymer matrix consisted of carbon nanotubes (CNTs), styrene sulfonic sodium (SSNa), β-cyclodextrin (β-CD)-grafted acrylamide, and ferrocene (Fc)-grafted acrylamide, with the incorporation of SSNa serving as the ionic source. On applying an external voltage, the ions accumulate on one side of the matrix, leading to localized swelling and bending of the structure. Therefore, a controllable and reversible actuation can be achieved by changing the applied voltage. The tensile strength of the SIPC was improved by over 300%, from 12 to 49 kPa, due to the reinforcement effect of the CNTs and the supramolecular host–guest interactions between the β-CD and Fc moieties. The inclusion of CNTs not only improved the tensile properties but also enhanced the ion mobility, which lead to a faster electromechanical response. The presented electro-responsive composite hydrogel shows a high potential for the development of robotic devices and soft smart components for sensing and actuating applications.

Keywords: supramolecular ionic polymer, single-walled carbon nanotube, composite hydrogel, electro-mechanical performance

1 Introduction

Hydrogels with smart functionalities, such as self-healing [1] and stimuli-responsive properties [2–4], have drawn wide research attention in a variety of applications, including therapeutics [5,6], robotics [7,8], and sensors [9]. Electroactive hydrogels (EAHs) are hydrophilic and electroactive materials with a three-dimensional molecular network, exhibiting reversible actuation in response to an electric field. Since electric fields can be easily applied and controlled, EAHs are considered as suitable candidates for the fabrication of the artificial muscles, sensors, actuators, and robotic devices that require low voltage for actuation [10–12]. Polyacrylamide (PAAM) and its copolymers have been widely used in preparing EAHs for artificial muscles and soft sensors due to the advantages of lightweight, low cost, designable physical and chemical properties, high water content, and biocompatible properties [13,14]. For example, Wang and colleagues prepared the polyanionic poly(2-acrylamido-2-methylpropanesulfonic acid-*co*-acrylamide) (AMPS-*co*-AAM) hydrogel walkers, which could walk and manipulate objects by applying a controlled DC voltage [15]. Li et al. prepared the electro-responsive poly(AMPS-*co*-AAM) by cross-linking triblock copolymer micelles [16]. However, the biggest problems of these hydrogels are weak mechanical

* **Corresponding author: Chak-Yin Tang,** Department of Industrial and Systems Engineering, The Hong Kong Polytechnic University, Hung Hom, Kowloon, Hong Kong, China, e-mail: cy.tang@polyu.edu.hk
* **Corresponding author: Fei-Peng Du,** Department of Industrial and Systems Engineering, The Hong Kong Polytechnic University, Hung Hom, Kowloon, Hong Kong, China; School of Materials Science and Engineering, Wuhan Institute of Technology, Wuhan, China, e-mail: hsdfp@163.com
Yun-Fei Zhang: Department of Industrial and Systems Engineering, The Hong Kong Polytechnic University, Hung Hom, Kowloon, Hong Kong, China; School of Materials Science and Engineering, Wuhan Institute of Technology, Wuhan, China
Ling Chen: Manufacturing, CSIRO, Private Bag 10, Clayton South, Vic 3169, Australia
Ka-Wai Yeung, Yuqing Dong, Wing-Cheung Law, Gary Chi-Pong Tsui: Department of Industrial and Systems Engineering, The Hong Kong Polytechnic University, Hung Hom, Kowloon, Hong Kong, China

strength and relatively slow response, which limits their application scope.

Development of novel composite materials is important for improving the material performance [17–19]. For instance, carbon nanomaterials have been widely used as a functional additive in polymers to improve the mechanical, electrical, and thermal properties of nanocomposites [20–23]. Recently, reports have indicated that the mechanical strength and electro-response characteristics of EAHs could be improved by adding electro-active components, such as graphene [24] and multi-walled carbon nanotubes (MWCNTs) [25], to the polymer matrix. Yang et al. reported that the mechanical and electro-response properties of the poly(AMPS-*co*-AAM) were improved by introducing reduced graphene oxide nanosheets [26]. Li et al. reported that the tensile strength of the PAAM hydrogels can be greatly improved by grafting MWCNTs on the polymer matrix [27]. Carbon nanotubes (CNTs) have excellent strength and thermal stability as well as high electrical conductivity [28], which make them promising as ideal electro-active components for rapid response actuators and devices that require high electrochemical stability [29–31]. However, incorporation of inorganic CNTs into polymer matrices is always problematic due to the poor solubility and low dispersibility of CNTs in water or organic solvents [32,33]. In this respect, much effort has been expended on the modification of CNTs through covalent [34,35] or non-covalent [36] strategies to improve their solubility and processability [37]. However, there has been sparse research investigating the influence of the single-walled carbon nanotubes (SWCNTs) concentration on the electro-response performance of the hydrogels.

Some research studies have been carried out to fabricate the actuating materials based on the supramolecular assembly of two individual hydrogels containing a β-cyclodextrin (β-CD) host and ferrocene (Fc) guest moieties [38,39]. This bilayer strip has shown a reversible bending behavior in response to a temperature change. The macroscopic self-assembly of the polymer hydrogels consisting of the β-CD and Fc gels was also investigated [40]. The β-CD gel adhered to the Fc gels through a host–guest interaction, achieving a strong adhesion strength. The results suggested that the supramolecular ion assembly between β-CD and Fc would be beneficial to the mechanical properties of the hydrogels. The supramolecular ion assembly of a copolymer containing β-CD and Fc moieties has also been studied and the redox-switchable properties of the copolymer have been confirmed in the electrochemical response of the Fc moieties [41], conferring voltage-controllable assembly and disassembly features to the samples [42].

In our study, the supramolecular ionic polymer–carbon nanotube composite (SIPC) hydrogels with good mechanical properties and electro-responsibility were successfully fabricated via *in situ* free radical polymerization based on styrene sulfonic sodium (SSNa), β-CD-grafted acrylamide, and Fc-grafted acrylamide. The influence of the supramolecular and carbon nanotube concentration on the structure, swelling behavior, thermal degradation, and mechanical properties and electromechanical performance of the composite hydrogels were investigated. The SIPC hydrogels showed a reversible electromechanical response in terms of bending behavior under the electric field. It was found that with the incorporation of the CNTs and the supramolecular ion assembly between the β-CD and the Fc, the SIPC showed an improved tensile strength without compromising the toughness. The electromechanical response time was also reduced with the addition of the CNTs.

2 Experimentation

2.1 Materials

Pristine SWCNTs (diameter 1–3 nm, length > 15 μm, purity > 83%) were purchased from Shenzhen Nanotech Port Co., Ltd (Shenzhen, China). Vinyl-functionalized single-wall carbon nanotubes (V-SWCNTs) (Figure 1), β-CD-grafted acrylamide (β-CD-AAM), and Fc-grafted acrylamide (Fc-AAM) were the starting materials for the fabrication of the SIPC, which were synthesized according to the literature [43,44]. Analytical acrylamide (AAM), *N*,*N*′-methylene-bis-acrylamide (MBAAM), SSNa, and ammonium peroxodisulfate (APS) were obtained from Sinopharm Chemical Reagent Co., Ltd (Beijing, China). All chemicals were directly used without further purification. Water was purified with UP-20 before use.

2.2 Preparation of SIPC hydrogel films for actuation

V-SWCNTs with different weight fractions (0, 0.25, 0.5, and 1 wt%) were dispersed in an aqueous reactant containing 85 mol% AAM, 14 mol% MBAAM, and 1 mol% SSNa. APS was then added as a thermal initiator in a mole ratio of 1:100 between the initiator and the reactant. The SIPCs with different compositions were prepared, and the details are shown in Table 1. SIPC-1 to

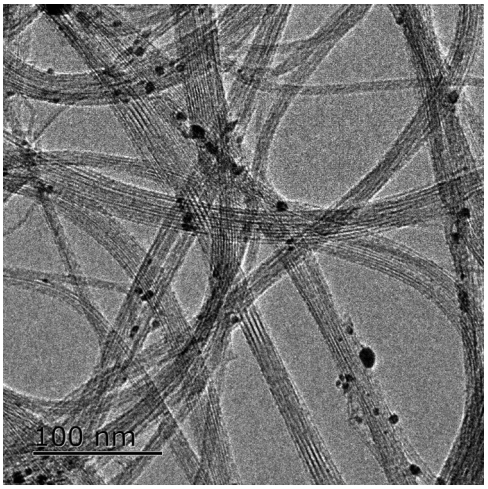

Figure 1: TEM image of V-SWCNTs.

SIPC-4 thin films containing different weight of SWCNT nanofillers were prepared by transferring the solution into a laboratory-made mold of dimensions 100 mm × 100 mm × 1 mm in a water bath at 40°C. The β-CD-AAM and Fc-AAM monomers (in 1:1 mole ratio) were mixed together to achieve a supramolecular ion assembly between the β-CD and Fc moieties. The mixture of β-CD-AAM/Fc-AAM was added as a host–guest monomer into the above aqueous reactant containing 1 wt% SWCNT and vigorously stirred at room temperature for 24 h to prepare SIPC-5. The mole ratio between the host–guest monomer and the reactant (excluding V-SWCNTs) was 8:100. The polymerization reaction was allowed to proceed for several minutes, and subsequently, the film was washed with dimethyl sulfoxide and deionized water. The samples were cut and trimmed into rectangular strips of 5 mm width and 40 mm length.

2.3 Morphology and compositional characterizations

The morphology of the samples was determined using a Zeiss SIGMA field-emission scanning electron microscope (FE-SEM, Germany). Fourier transform infrared (FTIR) spectra were obtained using an IR spectrometer (Nicolet 6700, USA) with an attenuated total reflectance attachment. Raman spectra were recorded for all the samples at ambient conditions using a Raman spectrometer (DXR, USA) with an excitation laser source at 633 nm. The X-ray diffraction (XRD) patterns at wide angles 2θ (from 10° to 90°) with Cu K_α radiation (λ = 1.54 Å) were obtained using a New D8-Advance/Bruker-AXS (Germany) powder X-ray diffractometer operating at 40 kV and 30 mA, a scanning rate of 6°/min, and a scanning step of 0.02. The thermogravimetric analysis (TGA) was performed using a thermo-gravimetric analyzer (STA449F3, Germany) at the heating rate of 20°C/min from 30 to 700°C in an argon flow (20 mL/min). The samples for SEM, IR, Raman, XRD, and TG test were first frozen for 24 h and then freeze-dried at −55°C in vacuum for 24 h.

2.4 Physical properties of SIPC hydrogels

The as-prepared composite hydrogels, with an initial weight m_0, were immersed in pure water, with the weight at time t (m_t), at room temperature. At different time intervals, the swelling ratio (w/w) was defined as $(m_t - m_0)/m_0$.

Tensile tests of the composite hydrogels were conducted with reference to the ASTM D638 standard, with slight modification [45]. Uniaxial tensile tests on rectangular hydrogel strips (50 mm × 10 mm × 1.0 mm) were performed on an Instron 5567 universal testing machine at a crosshead speed of 10 mm/min.

2.5 Electromechanical behavior

The electromechanical response of the hydrogels was studied under a direct current (DC) electric field using the setup shown in Figure 2. NaCl solution (50 mL, 1.0 mol/L) was poured into an organic glass box with two parallel carbon electrodes separated by 6.0 cm.

Table 1: Compositions of the prepared SIPC hydrogels

Samples	AAM (mol%)	MBAAM (mol%)	SSNa (mol%)	V-SWCNTs (wt%)	β-CD-AAM/Fc-AAM (wt%)
SIPC-1	85	14	1	0	0
SIPC-2	85	14	1	0.25	0
SIPC-3	85	14	1	0.50	0
SIPC-4	85	14	1	1.00	0
SIPC-5	85	14	1	1.00	1

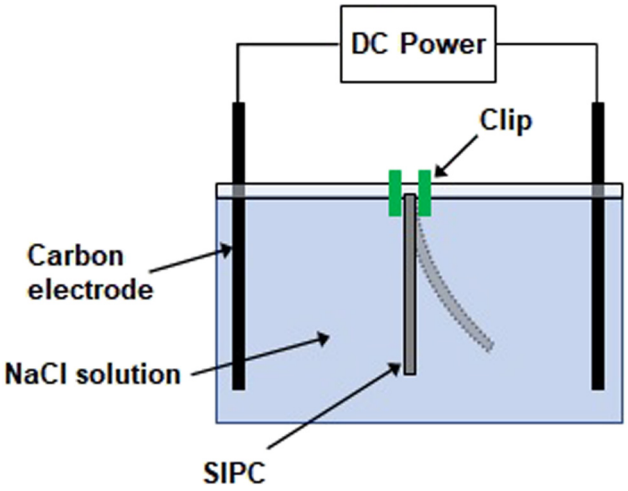

Figure 2: Illustration of the experimental setup for the electro-mechanical response test.

Before the experiment, the hydrogels were cut into strips of 50 mm (length) × 5 mm (width) × 1 mm (thickness). The SIPC hydrogel strip was fixed at one end with the other end immersed in a NaCl solution. The real-time response behavior was recorded by a digital camera, and the bending angle was measured by a protractor. The response speed of the SIPC samples was assessed by the change in the bending angle within the first 30 s after applying the electric potential.

3 Results and discussion

3.1 Preparation of SIPC

The new design of the SIPC hydrogel in this study is a chemical crosslinking network structural copolymer that consists of SSNa, AAM, MBAAM, β-CD-AAM, and Fc-AAM, as shown in Figure 3. In this copolymer, the SWCNTs are covalently attached to the polymer backbones. Due to the effect of electrostatic double layer of the SWCNTs, enhanced electromechanical performance can be achieved. Inside the SIPC hydrogel, SSNa provides the free sodium cations within the hydrogel. The supramolecular ion assembly between the β-CD and Fc moieties induces a reversible physical crosslinking of the monomers due to the non-covalent host–guest interaction. As a result, the integrity and mechanical properties of the hydrogel can be improved. In addition, Fc can be oxidized and dissociates with β-CD under different electrical charging conditions.

3.2 Characterizations of SIPC

The morphologies of SIPC-1, SIPC-4, and SIPC-5 were investigated by FE-SEM. As shown Figure 4a, no SWCNTs were observed in SIPC-1. Besides, within SIPC-4 and SIPC-5 (Figure 4b–d), which have the highest SWCNT content, the SWCNTs are well dispersed and they are interconnected to form 3D nanotube bundle networks (red arrow). The vinyl functionalization of the SWCNTs has shown good miscibility with the polymer matrix. Moreover, this result also shows that the incorporation of the supramolecular molecules does not affect the dispersibility of the SWCNTs. The high-magnification FE-SEM graphs of SIPC-5 (Figure 4d) show that the nanotube networks are tightly imbedded in the supramolecular matrix (white arrow), which plays an important role in the enhancement of the mechanical and electro-responsive properties of the SIPC.

FTIR spectra were used to characterize the functional groups of the SIPC hydrogels. As shown in Figure 4e, the peaks at 1,660 and 1,414 cm^{-1} correspond to the C=O and C–N stretching vibrations of the amide bond in the AAM units, respectively [46]. The peaks at 2,927 cm^{-1} and 2,862 cm^{-1} are ascribed to the C–H asymmetric and symmetric stretching vibrations of the main AAM units, respectively. In addition, there are strong absorption peaks between 1,020 and 1,500 cm^{-1}, corresponding to the polar groups, such as –NH, –OH, and C=O, present in the synthesized hydrogels, suggesting high water hydrophilicity of the SIPC hydrogels. Furthermore, all SIPC hydrogels showed characteristic peaks of the N–H asymmetric and symmetric stretching vibrations of the main AAM units at 3,435 and 3,195 cm^{-1}, without noticeable peaks for the vinyl group, indicating that *in situ* free radical polymerization has been successfully conducted.

Raman spectra were used to characterize the defects and the disordered structures of the carbon-based materials. The Raman spectra of the SIPC hydrogels are shown in Figure 4f. The peaks at 1,332 cm^{-1} (D band) and 1,579 cm^{-1} (G band) are, respectively, attributed to the disordered graphite structure or sp^3-hybridized carbons of the nanotubes and splitting of the E_{2g} stretching mode of the graphite, reflecting the structural intensity of the sp^2-hybridized carbon atoms. It can be seen that, after the grafting copolymerization with SSNa and acrylamide monomers, the intensity of the D band becomes much higher than that of the G band. This indicates a higher extent of disorder in the CNTs [47,48]. Therefore, the G band is not obvious in the Raman spectrum. The peak at 1,603 cm^{-1} is ascribed to the C=C stretching vibration of SSNa.

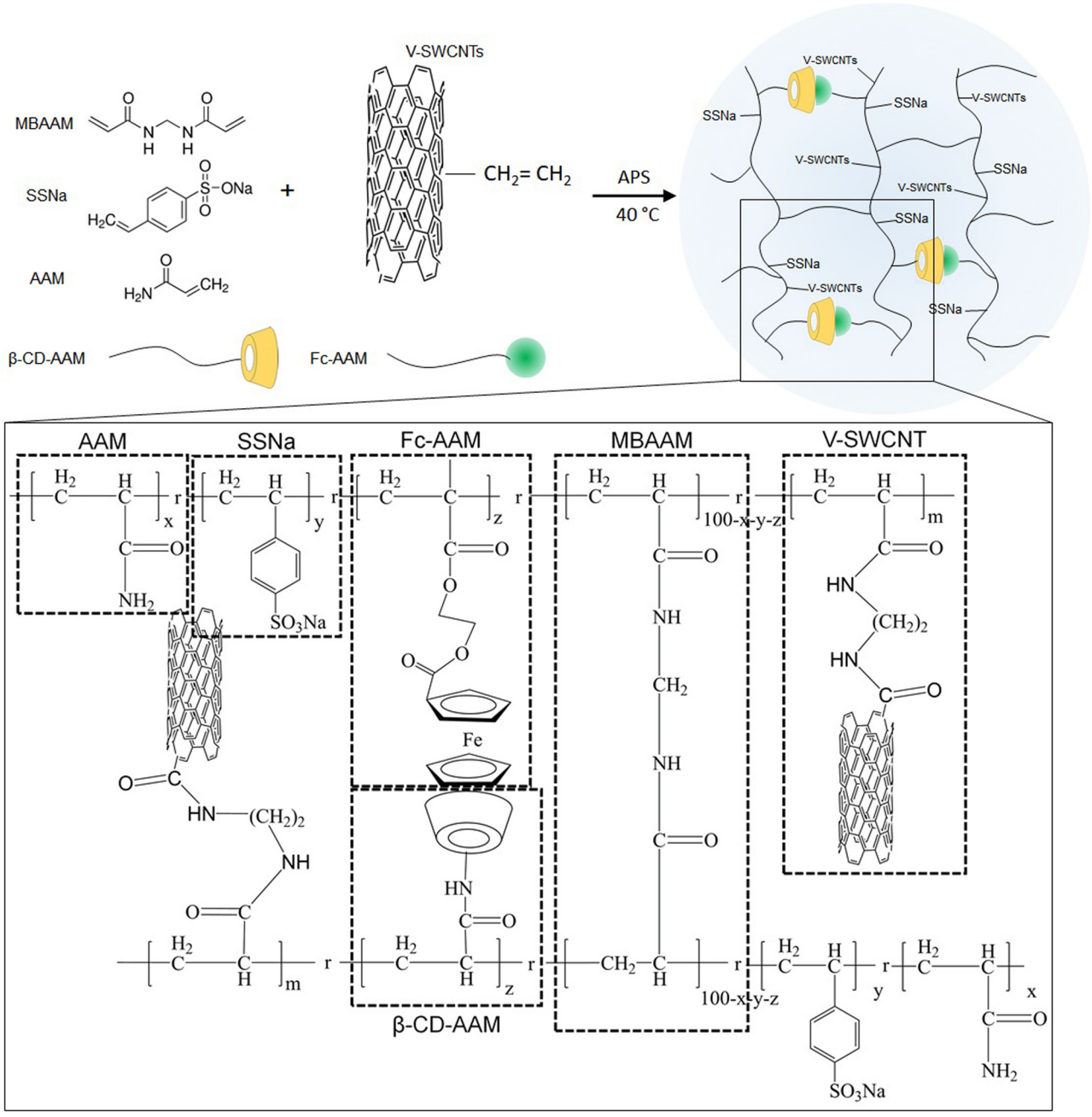

Figure 3: Chemical structure of the SIPC hydrogels.

Figure 4g shows the XRD patterns of different SIPC samples. The XRD patterns of the V-SWCNTs exhibit an obvious peak at $2\theta = 26.7°$. This peak is also observed in the XRD patterns of SIPC-4 and SIPC-5, which correspond to the (002) peak of the SWCNTs. This is mainly attributed to the intertube structure (outer wall contacts) of the individual SWCNTs [49]. However, due to the low SWCNTs loading ratio, this peak is not observed in SIPC-2 and SIPC-3. Besides, no other obvious sharp peaks are observed, indicating the amorphous nature of the SIPC hydrogel films.

CNTs have been widely used to improve the thermal stability of the polymeric nanocomposites [50]. Here, TGA was used to study the effect of SWCNTs and host–guest molecules on the thermal degradation behavior of the SIPC hydrogels. As shown in Figure 4(h and i), all SIPC samples exhibit a slight weight loss between 100 and 200°C, which is mainly due to the water loss, including free water and combined water. With an increasing amount of SWCNTs from 0 to 0.5 wt% (SIPC-1 to SIPC-3), the initial degradation temperature of the samples is increased from 150 to 300°C,

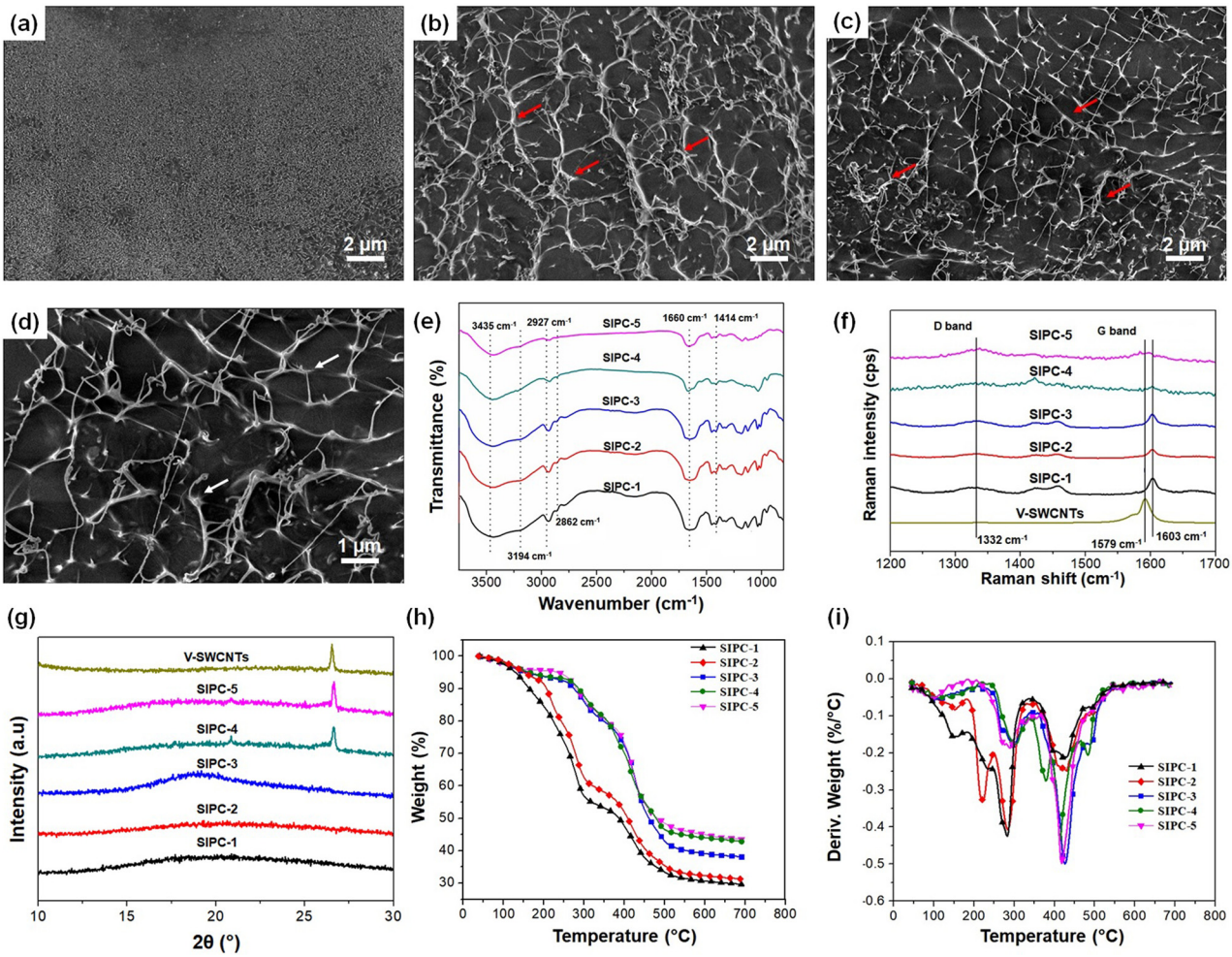

Figure 4: FE-SEM images of (a) SIPC-1, (b) SIPC-4, and (c and d) SIPC-5 (the red arrows indicate the SWCNT bundle networks and the white arrows show the embedment of SWCNTs in the polymer matrix). (e) FTIR spectra, (f) Raman spectra, (g) XRD patterns, (h) TG curves, and (i) DTG curves of the SIPC hydrogels.

indicating the enhancement of thermal stability. It can also be seen that the higher the amount of SWCNTs, the higher is the char yield of the SIPC. The interconnected SWCNT networks in the SIPC hydrogel act as a reinforcement that can hinder the propagation of cracks and promote the formation of stable char layers, thereby efficiently protecting the underlying polymeric materials from degradation. In addition, the incorporation of host–guest molecules has less influence on the thermal stability of the SIPC.

3.3 Swelling behavior and mechanical properties

The swelling ratios of the SIPC samples in water within 2 h at room temperature (25°C) are plotted in Figure 5a. The swelling of the hydrogels almost reaches saturation within 2 h. Most of the SIPC samples exhibit a high swelling ratio in water due to the incorporation of SSNa. However, with the increasing SWCNT content, the swelling ratio of the SIPC hydrogels decreased gradually from 1.2 (w/w) to around 0.3 (w/w). This is attributed to the formation of the SWCNT network, as shown in FE-SEM, which limits the swelling of the SPIC. Compared with SIPC-4, the swelling ratio of SIPC-5 is lower. This suggests that the swelling ratio of the SIPC hydrogels is reduced by the supramolecular ion assembly of the β-CD and Fc moieties.

Tensile tests were conducted to evaluate the mechanical properties of the SIPC hydrogels, and the results are shown in Figure 5b. It is obvious that the tensile properties of the SWCNT-incorporated SIPC hydrogels are improved over the SWCNT-free hydrogel (SIPC-1). Noticeably, as the SWCNT content increased from 0.0 to 1.0 wt%, the tensile strengths of the composite hydrogels

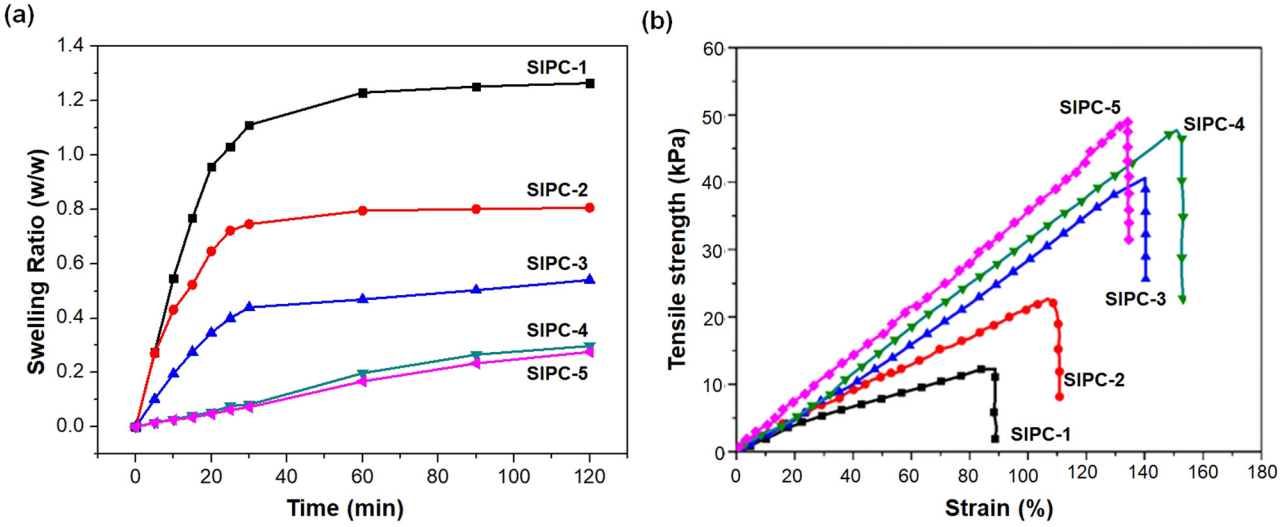

Figure 5: (a) Swelling ratio versus time and (b) the tensile stress–strain curves of the SIPC hydrogels.

increased significantly from 12 kPa (SIPC-1) to 47 kPa (SIPC-4). The tensile strength of the SIPC hydrogels can be effectively regulated without compromising the toughness by adjusting the SWCNT content. The enhancement of the tensile property of the SWCNT-containing SIPC hydrogels is due to (i) the well-dispersed SWCNTs in the hydrogel network by means of free radical graft polymerization; (ii) the strengthened hydrogels by the nano-reinforcement effect of the SWCNTs; and (iii) the toughening effect of the functionalized SWCNTs [51]. Not only the vinyl functionalization of the SWCNTs improves the dispersibility within the polymer matrix but also the covalent functionalization enhances the interfacial strength and the adhesion between the SWCNTs and the polymer [48]. During the tensile test, the deformation of the polymer composite can lead to polymer chain movement and bond breakage. With the presence of covalently bonded SWCNTs, the applied load can be effectively transferred across the interface between the SWCNTs and the polymer matrix, thereby improving the tensile properties of the polymer composite [52]. Among all the prepared samples, SIPC-5 exhibited the highest tensile strength of 49 kPa, with an elastic modulus of 36.3 kPa. Although the CNT content of SIPC-4 and SIPC-5 are the same, SIPC-5 shows higher tensile strength and lower strain. This is due to the addition of the host–guest molecules β-CD-AAM and Fc-AAM. The supramolecular host–guest interaction between the β-CD and Fc moieties serves as additional crosslinking sites, thereby enhancing the tensile strength of the nanocomposite but reducing the strain under tension. Moreover, compared with a previously reported bilayer EAH with an estimated elastic modulus of 19.9 kPa [43], the SIPC-5 hydrogel has shown an 82% improvement in the tensile properties.

3.4 Electro-mechanical behavior

Under an applied electric potential of 10 V, the SIPC hydrogel films showed bending behavior. According to the previous reports and the actuation performance experiments, the bending mechanism of the SIPC hydrogels is derived from the osmotic pressure difference on the basis of Flory–Rehner theory due to the distribution of mobile ions under the electric field (Figure 6a) [4]. As the sulfonic acid group on SSNa is fixed on the polymer backbone, only sodium in the form of mobile ions can move around inside the SIPC hydrogel. When an external DC electric field is applied, the mobile ions migrate toward their counter-electrode. Therefore, a higher number of sodium ions move to the side closest to the cathode within the SIPC. This creates an osmotic pressure (π) difference across the SIPC hydrogel, which is associated with the ion concentration gradient. Due to the charge migration within the hydrogel, the osmotic pressure at the interface near the anode becomes larger than that at the cathode. Therefore, the composite hydrogel swells on the anode side while shrinking at the opposite side, and as a result, the hydrogels bend toward the cathode side, as shown in Figure 6b.

Due to the intrinsic properties of the SWCNTs, including the quantum chemical and electrostatic double-layer effect, they are promising materials for

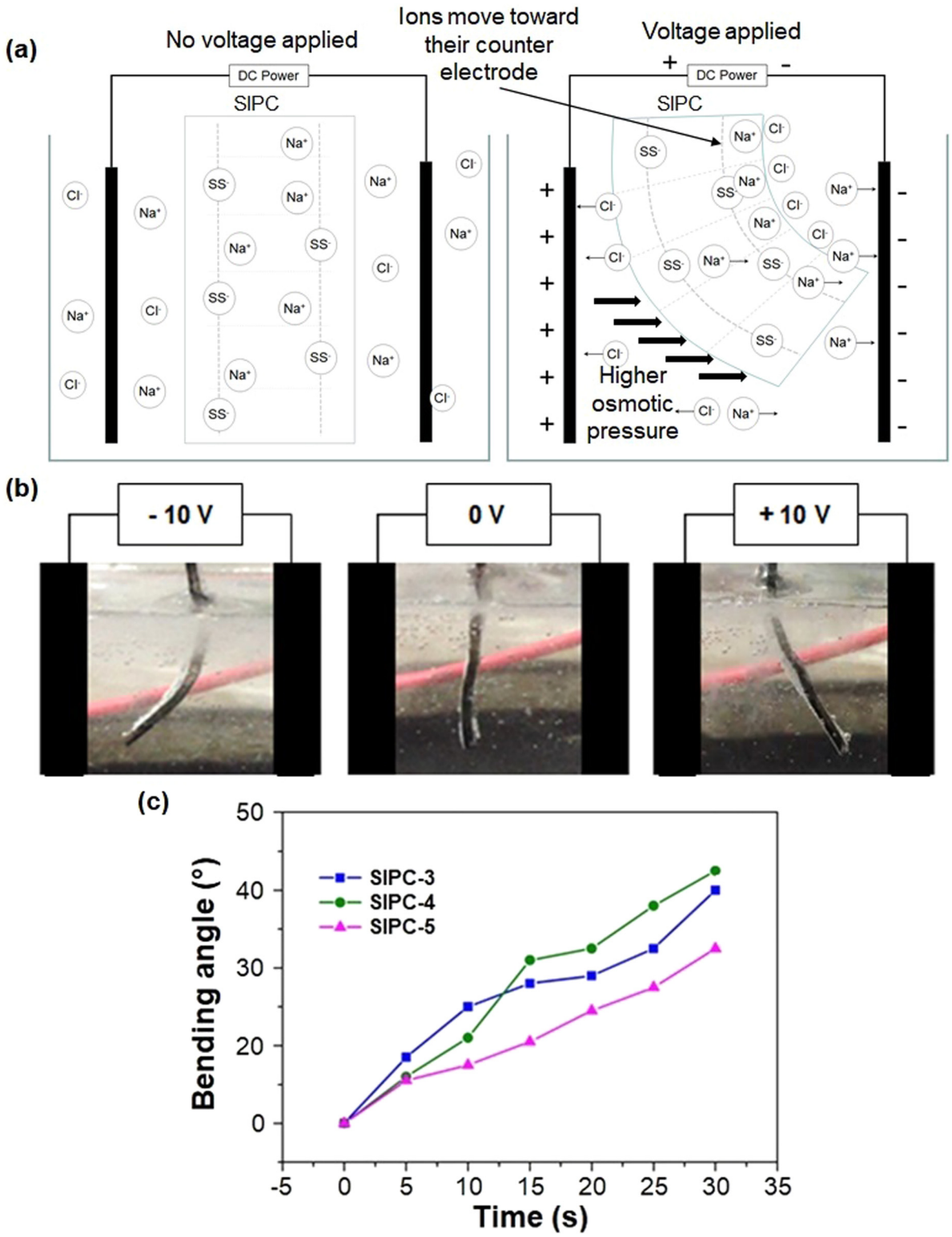

Figure 6: (a) Illustration of the bending mechanism and (b) bending of the SIPC-4 hydrogel under applied voltage. (c) The electromechanical response of the SIPC samples.

electromechanical actuators [53]. The SWCNTs within the SIPC hydrogels may facilitate the movement of ions and the formation of an ion concentration gradient [54]. As a result, a higher rate of change in the osmotic pressure difference can be achieved. It could enhance the electromechanical response of the SIPC hydrogels [4]. Therefore,

the electromechanical properties of the SIPC hydrogel can be enhanced by increasing the SWCNT content. This is proven by the electromechanical response of the SIPC hydrogel, as shown in Figure 6c. The deflection response time of the SIPC hydrogels with 0.5 and 1 wt% SWCNTs at 10 V were recorded. As the SWCNT content increased, the response time was reduced by over 2 s to reach 55° bending. A faster actuation can be achieved by optimizing the SWCNT content in the SIPC hydrogels. When the supramolecular β-CD and Fc moieties (β-CD-AAM/Fc-AAM) were introduced into the hydrogels, the response speed was lowered (SIPC-5). This can be attributed to the hardening effect given by the non-covalent host–guest interaction, which serves as the crosslinking sites between the supramolecular moieties within SIPC-5. Further study is required to elucidate the mechanism of this hardening effect. In fact, the enhanced mechanical properties obtained in SIPC-5 provides a good opportunity to develop electro-responsive micro-actuators with a high output force.

4 Conclusions

In this study, novel electro-responsive SIPC hydrogels based on SSNa, β-CD-AAM, Fc-AAM, and SWCNTs with enhanced electromechanical performance have been synthesized. With the inclusion of SWCNTs and the supramolecular moieties (β-CD and Fc), the tensile strengths of the samples have been improved. In NaCl aqueous solutions, the SIPC hydrogels have shown a reversible bending motion and the direction can be controlled by the electric field. Moreover, a faster electromechanical response can be achieved by increasing the SWCNT content. Due to the enhanced mechanical properties and faster response time of the SIPC, we believe that the developed materials possess high potential for application in the design and prototyping of smart micro-actuation systems.

Acknowledgments: This work was substantially supported by a grant from the Research Grants Council of the Hong Kong Special Administrative Region, China (Project No. PolyU 15207215), and partially supported by a grant from the Research Committee of the Hong Kong Polytechnic University (Project code G-YBVX).

Conflict of interest: The authors declare no conflict of interest regarding the publication of this paper.

References

[1] Koetteritzsch J, Schubert US, Hager MD. Triggered and self-healing systems using nanostructured materials. Nanotechnol Rev. 2013;2:699–723.
[2] Lv C, Sun XC, Xia H, Yu YH, Wang G, Cao XW, et al. Humidity-responsive actuation of programmable hydrogel microstructures based on 3D printing. Sens Actuat B-Chem. 2018;259:736–44.
[3] Ma C, Le X, Tang X, He J, Xiao P, Zheng J, et al. A multiresponsive anisotropic hydrogel with macroscopic 3d complex deformations. Adv Funct Mater. 2016;26:8670–76.
[4] Liu Q, Dong Z, Ding Z, Hu Z, Yu D, Hu Y, et al. Electroresponsive homogeneous polyelectrolyte complex hydrogels from naturally derived polysaccharides. ACS Sustain Chem Eng. 2018;6:7052–63.
[5] Miao Y, Lu J, Yin J, Zhou C, Guo Y, Zhou S. Yb^{3+}-containing chitosan hydrogels induce B-16 melanoma cell anoikis via a Fak-dependent pathway. Nanotechnol Rev. 2019;8:645–60.
[6] Luan C, Liu P, Chen R, Chen B. Hydrogel based 3D carriers in the application of stem cell therapy by direct injection. Nanotechnol Rev. 2017;6:435–48.
[7] Higashi K, Miki N. A self-swimming microbial robot using microfabricated nanofibrous hydrogel. Sens Actuat B-Chem. 2014;202:301–6.
[8] Li H, Go G, Ko SY, Park JO, Park S. Magnetic actuated pH-responsive hydrogel-based soft micro-robot for targeted drug delivery. Smart Mater Struct. 2016;25:027001.
[9] Zhang YZ, Lee KH, Anjum DH, Sougrat R, Jiang Q, Kim H, et al. MXenes stretch hydrogel sensor performance to new limits. Sci Adv. 2018;4:eaat0098.
[10] Liao M, Wan P, Wen J, Gong M, Wu X, Wang Y, et al. Wearable, healable, and adhesive epidermal sensors assembled from mussel-inspired conductive hybrid hydrogel framework. Adv Funct Mater. 2017;27:1703852.
[11] Browe DP, Wood C, Sze MT, White KA, Scott T, Olabisi RM, et al. Characterization and optimization of actuating poly (ethylene glycol) diacrylate/acrylic acid hydrogels as artificial muscles. Polymer. 2017;117:331–41.
[12] Srisawasdi T, Petcharoen K, Sirivat A, Jamieson AM. Electromechanical response of silk fibroin hydrogel and conductive polycarbazole/silk fibroin hydrogel composites as actuator material. Mater Mater Sci Eng C Mater. 2015;56:1–8.
[13] Bassil M, Davenas J, El Tahchi M. Electrochemical properties and actuation mechanisms of polyacrylamide hydrogel for artificial muscle application. Sens Actuat B-Chem. 2008;134:496–501.
[14] Bassil M, El Tahchi M, Souaid E, Davenas J, Azzi G, Nabbout R. Electrochemical and electromechanical properties of fully hydrolyzed polyacrylamide for applications in biomimetics. Smart Mater Struct. 2008;17:055017.
[15] Yang C, Wang W, Yao C, Xie R, Ju XJ, Liu Z, et al. Hydrogel walkers with electro-driven motility for cargo transport. Sci Rep. 2015;5:13622.
[16] Li YF, Sun YN, Xiao Y, Gao GR, Liu SH, Zhang JF, et al. Electric field actuation of tough electroactive hydrogels cross-linked by functional triblock copolymer micelles. ACS Appl Mater Inter. 2016;8:26326–31.
[17] Wang H, Nie S, Li H, Ali R, Fu J, Xiong H, et al. 3D hollow quasi-graphite capsules/polyaniline hybrid with a high performance

for room-temperature ammonia gas sensors. ACS Sens. 2019;4:2343–50.
[18] Jian X, Tian W, Li J, Deng L, Zhou Z, Zhang L, et al. High-temperature oxidation-resistant $ZrN_{0.4}B_{0.6}$/SiC nanohybrid for enhanced microwave absorption. ACS Appl Mater Inter. 2019;11:15869–80.
[19] Guo Y, Jian X, Zhang L, Mu C, Yin L, Xie J, et al. Plasma-induced FeSiAl@Al_2O_3@SiO_2 core–shell structure for exceptional microwave absorption and anti-oxidation at high temperature. Chem Eng J. 2020;384:123371.
[20] Lamanna G, Battigelli A, Menard-Moyon C, Bianco A. Multifunctionalized carbon nanotubes as advanced multimodal nanomaterials for biomedical applications. Nanotechnol Rev. 2012;1:17–29.
[21] Zhang H, Li X, Qian W, Zhu J, Chen B, Yang J, et al. Characterization of mechanical properties of epoxy/nanohybrid composites by nanoindentation. Nanotechnol Rev. 2020;9:28–40.
[22] Gao M, Zheng F, Xu J, Zhang S, Bhosale SS, Gu J, et al. Surface modification of nano-sized carbon black for reinforcement of rubber. Nanotechnol Rev. 2019;8:405–14.
[23] Lei M, Chen Z, Lu H, Yu K. Recent progress in shape memory polymer composites: methods, properties, applications and prospects. Nanotechnol Rev. 2019;8:327–51.
[24] Qiao K, Guo S, Zheng Y, Xu X, Meng H, Peng J, et al. Effects of graphene on the structure, properties, electro-response behaviors of GO/PAA composite hydrogels and influence of electro-mechanical coupling on BMSC differentiation, Mater Sci Eng C Mater. 2018;93:853–63.
[25] Mehrali M, Thakur A, Pennisi CP, Talebian S, Arpanaei A, Nikkhah M, et al. Nanoreinforced hydrogels for tissue engineering: biomaterials that are compatible with load-bearing and electroactive tissues. Adv Mater. 2017;29:1603612.
[26] Yang C, Liu Z, Chen C, Shi K, Zhang L, Ju XJ, et al. Reduced graphene oxide-containing smart hydrogels with excellent electro-response and mechanical properties for soft actuators. ACS Appl Mater Inter. 2017;9:15758–67.
[27] Li Z, Tang M, Dai J, Wang T, Bai R. Effect of multiwalled carbon nanotube-grafted polymer brushes on the mechanical and swelling properties of polyacrylamide composite hydrogels. Polymer. 2016;85:67–76.
[28] Zhang D, Miao M, Niu H, Wei Z. Core-spun carbon nanotube yarn supercapacitors for wearable electronic textiles. ACS nano. 2014;8:4571–79.
[29] Terasawa N, Asaka K. High-performance cellulose nanofibers, single-walled carbon nanotubes and ionic liquid actuators with a poly(vinylidene fluoride-*co*-hexafluoropropylene)/ionic liquid gel electrolyte layer. RSC Adv. 2019;9:8215–21.
[30] Ozarkar S, Jassal M, Agrawal AK. pH and electrical actuation of single walled carbon nanotube/chitosan composite fibers. Smart Mater Struct. 2008;17:055016.
[31] Hines L, Petersen K, Lum GZ, Sitti M. Soft actuators for small-scale robotics. Adv Mater. 2017;29:1603483.
[32] Kwon DJ, Shin PS, Kim JH, DeVries KL, Park JM. Evaluation of optimal dispersion conditions for CNT reinforced epoxy composites using cyclic voltammetry measurements. Adv Compos Mater. 2017;26:219–27.
[33] Terasawa N, Asaka K. High-performance graphene oxide/vapor-grown carbon fiber composite polymer actuator. Sens Actuat B-Chem. 2018;255:2829–37.
[34] Dinesh B, Bianco A, Ménard-Moyon C. Designing multimodal carbon nanotubes by covalent multi-functionalization. Nanoscale. 2016;8:18596–611.
[35] Duan Q, Wang S, Wang Q, Li T, Chen S, Miao M, et al. Simultaneous improvement on strength, modulus, and elongation of carbon nanotube films functionalized by hyperbranched polymers. ACS Appl Mater Inter. 2019;11:36278–85.
[36] Bilalis P, Katsigiannopoulos D, Avgeropoulos A, Sakellariou G. Non-covalent functionalization of carbon nanotubes with polymers. RSC Adv. 2014;4:2911–34.
[37] Mallakpour S, Soltanian S. Surface functionalization of carbon nanotubes: fabrication and applications. RSC Adv. 2016;6:109916–35.
[38] Zhang J, Wu J, Sun J, Zhou Q. Temperature-sensitive bending of bigel strip bonded by macroscopic molecular recognition. Soft Matter. 2012;8:5750–52.
[39] Nakahata M, Takashima Y, Hashidzume A, Harada A. Redox-generated mechanical motion of a supramolecular polymeric actuator based on host–guest interactions. Angew Chem Int Ed Engl. 2013;52:5731–35.
[40] Nakahata M, Takashima Y, Harada A. Redox-responsive macroscopic gel assembly based on discrete dual interactions. Angew Chem Int Ed Engl. 2014;53:3617–21.
[41] Szillat F, Schmidt BVKJ, Hubert A, Barner-Kowollik C, Ritter H. Redox-switchable supramolecular graft polymer formation via ferrocene-cyclodextrin assembly. Macromol Rapid Commun. 2014;35:1293–300.
[42] Yuan Z, Wang J, Wang Y, Zhong Y, Zhang X, Li L, et al. Redox-controlled voltage responsive micelles assembled by non-covalently grafted polymers for controlled drug release. Macromolecules. 2019;52:1400–7.
[43] Zhang YF, Du FP, Chen L, Law WC, Tang CY. Synthesis of deformable hydrogel composites based on Janus bilayer multi-walled carbon nanotubes/host–guest complex structure, Compos. Part B-Engineering. 2019;164:121–8.
[44] Du FP, Wu KB, Yang YK, Liu L, Gan T, Xie XL. Synthesis and electrochemical probing of water-soluble poly(sodium 4-styrenesulfonate-*co*-acrylic acid)-grafted multiwalled carbon nanotubes. Nanotechnology. 2008;19:085716.
[45] Jing Z, Zhang Q, Liang YQ, Zhang Z, Hong P, Li Y. Synthesis of poly(acrylic acid)-Fe^{3+}/gelatin/poly(vinyl alcohol) triple-network supramolecular hydrogels with high toughness, high strength and self-healing properties. Polym Int. 2019;68:1710–21.
[46] Dutta S, Biswas G, Dhara D. Nanocomposite hydrogels for selective removal of cationic dyes from aqueous solutions. Polym Eng Sci. 2016;56:776–85.
[47] Jorio A, Pimenta MA, Souza AG, Saito R, Dresselhaus G, Dresselhaus MS. Characterizing carbon nanotube samples with resonance Raman scattering. N J Phys. 2003;5:1–17.
[48] Chen J, Yan L, Song W, Xu D. Interfacial characteristics of carbon nanotube-polymer composites: a review. Compos Part A-Appl S. 2018;114:149–69.
[49] Futaba DN, Yamada T, Kobashi K, Yumura M, Hata K. Macroscopic wall number analysis of single-walled, double-walled, and few-walled carbon nanotubes by X-ray diffraction. J Am Chem Soc. 2011;133:5716–19.
[50] Behdinan K, Moradi-Dastjerdi R, Safaei B, Qin Z, Chu F, Hui D. Graphene and CNT impact on heat transfer response of nanocomposite cylinders. Nanotechnol Rev. 2020;9:41–52.

[51] Hsieh T, Kinloch A, Taylor A, Kinloch I. The effect of carbon nanotubes on the fracture toughness and fatigue performance of a thermosetting epoxy polymer. J Mater Sci. 2011;46:7525.
[52] Lee HF, Yu HH. Study of electroactive shape memory polyurethane–carbon nanotube hybrids. Soft Matter. 2011;7:3801–07.
[53] Baughman RH, Cui C, Zakhidov AA, Iqbal Z, Barisci JN, Spinks GM, et al. Carbon nanotube actuators. Science. 1999;284:1340–44.
[54] Park C, Kang JH, Harrison JS, Costen RC, Lowther SE. Actuating single wall carbon nanotube–polymer composites: intrinsic unimorphs. Adv Mater. 2008;20:2074–79.